Frontiers in Heat and Mass Transfer (FHMT), 19, 31 (2022)
DOI: 10.5098/hmt.19.31

Global Digital Central
ISSN: 2151-8629

Frontiers in Heat and Mass Transfer

Available at www.ThermalFluidsCentral.org

FLOW DIRECTION EFFECTS ON TEMPERATURE DISTRIBUTION OF LI-ION CYLINDRICAL BATTERY MODULE WITH WATER/FERROFLUID AS COOLANTS

Sarawut Sirikasemsuk[a], Songkran Wiriyasart[a], Nittaya Naphon[b], Paisarn Naphon[a,*]

[1]*Thermo-Fluid and Heat Transfer Enhancement Lab. (TFHT), Department of Mechanical Engineering, Faculty of Engineering, Srinakharinwirot University, 63, Rangsit-Nakhornnayok Rd., Ongkharak, Nakhorn-Nayok, 26120, Thailand*
[2]*Department of Pharmaceutical Chemistry, Faculty of Pharmacy, Srinakharinwirot University, 63 Rangsit-Nakhornnayok Rd., Ongkharak, Nakhorn-Nayok, 26120, Thailand*

ABSTRACT

This paper investigates the working fluid with different flow directions on the battery management cooling system with de-ionized water and ferrofluid (0.015%by volume). The pack of batteries with two different coolant directions (Models I, II) used in the present study with sixty Li-ion cylindrical cells (25.2V and 30A) are tested under the trickle method for charged process and constant ampere for the discharged process to consider the battery module temperature distribution and cooling performance. The uniform temperatures of the battery pack significantly affect the long lifecycle and thermal performance. It is found that average temperatures are nearly constant at about 28.5°C and 29.65°C for models I and II, respectively. Decreasing the maximum temperature of the pack and the temperature gradient across the cell results in the decreasing reverse effect of the cell. In addition, the cooling model I gives the temperature gradient across the cell less than those from model II. In addition, the improved thermal physical properties of the coolant (Ferrofluid) significantly affect the battery pack decreasing operating temperature, compared with de-ionized water. However, the cooling system optimized condition, including the battery module with different operating conditions on a large scale, has been done for more extensive thermal performance and a more significant long lifecycle.

Keywords: *EV battery module; thermal cooling performance; ferrofluid*

1. INTRODUCTION

The batteries have been continuously developed from the lead-acid types to Nickel-based types and then now Li-ion batteries (Chen et al., 2016), which the Lithium-based types have many different cathode materials. For ideal, the battery charging process is performed at 100% state of charge (SOC) and 0%SOC for the discharging process. However, it has performed 90%SOC for the charged condition and 20% SOC for the discharged condition for safety. For the charging process, the average temperature of the battery should be between 0-45°C and 20-60°C for the discharging process. The thermally stable $LiMn_2O_4$ is more than $LiCoO_2$ for the battery using 500 cycles, and the cell capacity loss of about 12.91% (Chen et al. 2017).

The cylindrical shape battery is designed to mimic the battery and internally created roll alternating with stainless steel and mica layers. The cylindrical cell density module is about 1593 kg/m^3. This result is similar to the 18650 types (Spinner et al., 2016), which have an operating temperature of 20–40°C. However, under the thermal runaway effect, the temperature can be increased over 80°C (Deng et al., 2018). The rising temperature is still lower than 3°C (Jaguemont et al., 2018) for the fast-charged condition. Energy efficiency for the fast charging two-stage constant current process with high-low is better than the two-stage constant current with low-high and standard one-stage constant current (Xu et al., 2018). The status stage of the charged condition is determined from the remaining time of discharged condition (Chen et al., 2019). For the charged condition, the maximum current is used 6.7 times the total current (Amietszajew et al., 2016). The main topic of research on battery Li-ion focuses on safety without thermal runaway (Abada et al., 2016). The properties of the cylindrical cells are different between the radial and axial direction anisotropic (Drake et al., 2014).

The BTMS has research and experiment to control the temperature with air, water, other liquids, and phase change material (PCM) for cooling batteries used method direct or indirect. The BTMS can be protected from the temperature rise to the critical point. This may be caused to thermal runaway. Appropriate BTMS will increase the efficiency of electric vehicle batteries (Liu et al., 2017). The battery thermal runaway has an enormous effect on EVs working efficiency. This effect is not suitable for the battery thermal management system or electrochemical short-circuits, such as a controlled temperature lower than 110°C of $LiFePO_4$ battery (Wang et al., 2012). Concept three-level of the thermal runaway hazard is mechanical, electrical, and thermal abuse to reduce this hazard of smoke, fire, and explosion (Feng et al., 2018). Larsson et al., (2018) experimentally studied the Graphite-$LiCoO_2$ battery has thermal runaway risen at temperature 190°C. While experiment test with LiO_2 graphite battery has thermal runaway growth in environmental temperature start 150°C (Ren et al., 2018), the thermal runaway hazard with compression battery (Sheikh et al., 2017), and with phase change materials (Wilke et al., 2017). In the $LiCoO_2$ battery test at an environmental temperature of 80°C in different conditions of SOC, the results show that 100% SOC lowest onset is thermal runaway risen (Taniguchi et al., 2019), and battery deterioration can increase the thermal runaway (Parhizi et al., 2017) when the increasing battery temperature causes the reducing electric power to 75% (Feng et al., 2015). Also, thermal runaway is a chain chemical reaction that causes increasing cell temperature. Many researchers have solved this problem by designing a cooling system to protect battery thermal runaway with many different techniques, including a mini-channel heat sink, graphite composite sheet, and aluminum extrusion (Yuan et al., 2019). The BTMS has a fluent effect on working efficiency and long lifetime. The battery cooling systems are divided into three groups according to the coolant flowing in the system.

Air cooling is the technique in which air flows through an electric vehicle battery module. Researchers have designed the air cooler by

* Corresponding author. Email: paisarnn@g.swu.ac.th

Global Digital Central
ISSN: 2151-8629

forcing air to flow through space under conditions such as the inlet air corner, outlet air corner, air channel size, and outlet air channel size. Research conducted on the air pattern that flows through the space between the batteries (Cheng et al., 2018; Xie et al., 2017; Hong et al., 2018; Chen et al., 2017;2017;2018; Sun et al., 2014; Shahid et al., 2018; Chen et al., 2016) includes the length of the pipe, pipe diameter, the gap between the pipe and battery, and the amount of pipe by adjusting the speed, flow rate and air volume that feed into the system (Mousavi et al., 2011, Lu et al., 2016;2018; Kitagawa et al., 2014; Saw et al., 2017). Bolsinger et al., (2019) studied on the electrical impact test determines the electrical voltage, the current used for the C-Rate test, and the observation of the battery module for the SOC energy content. This also includes the study for achieving low cost and use for air cooling in electric vehicles (Erb et al., 2017). Most researchers focus on thermal management efficiency in an air-cooling system to determine the highest operating temperature, the uniform temperature of the battery, and the average temperature. The maximum temperature is controlled not to exceed 40ºC, the energy used is reduced, and the costs are reduced. U-type flow allows for up to a 70% temperature difference and optimized formulation.

Liquid cooling allows fluid to flow through the pipe or the flow channel for a cooling system. The equipment used may be an auxiliary material or a device made as a model with both a battery and a fluid flow channel. For the materials, researchers have tried using aluminum blocks (Rao et al., 2017), aluminum foams (Saw et al., 2017), aluminum tubing in combination with flexible graphite (Zhang et al., 2017), or carbon fiber composites (Pety et al., 2017). Electrical testing was performed with the C-Rate current at various rates (Zhao et al., 2018; Li et al., 2018; Malik et al., 2018) in conjunction with the adjustment of the mechanical parameters, which are flow rate or mass flow rate (Zhao et al., 2015), pipe contact surface area, or pipe heat exchanger area along the pipe length (Jiaqiang et al., 2018). Additionally, the number of pipes (Jarrett et al., 2014), size of pipes (Tan et al., 2018), including the use of nanofluids (Wiriyasart et al., 2020) were implemented to increase thermal cooling efficiency.

Aside from air and liquid cooling independently, both systems are also brought to work together by researchers who have designed a device for cooling the battery by relying on forced-flowing cool gas and cold liquid and analyzed from numerical method computational flow dynamics to find forced-flowing cool gas. The turbulence of the cold gas will affect the cooling efficiency. Compared to the vacuum cooling method (Wang et al., 2017), the battery generates an overall heat of 576 watts. The type of cooling system has significantly increased the cooling performance. Energy consumption for an air-cooling system is 2-3 times more than liquid cooling. The cooling fins will improve the system weight by more than 40%. The indirect liquid is the best for decreasing the operating temperature. Although the cooling efficiency of an indirect approach is less than that of a direct liquid system, it is only marginally less while proving to be more practical (Chen et al., 2016). In liquid cooling, fluid efficiency can be improved by adding nanoparticles to increase heat exchange efficiency (Wang et al., 2017). Recently, the work on lithium-ion battery thermal behavior has been reviewed (Galatro et al., 2020; Singh et al., 2021). Next, Ghiji et al., (2021) experimentally studied the thermal behavior of the electrolyte using a calorimeter and a Bunsen burner as a precursor to examining the effectiveness of a water mist suppression system in extinguishing a lithium-ion battery pack. Budiman et al., (2022) experimentally visualized the streamwise development of counter-rotating vortices from the electric vehicle battery module. Zhang et al., (2022) studied the self-forming air-cooled battery rack.

As reviewed above, there are many cooling methods to reduce thermal accumulation. The heat transfer ability depends on the properties and fluid flow characteristics of the working fluid, air, and liquid systems. Besides, the physical properties improvement of working fluid flowing through the cooling system has received much attention, with higher heat transferability. Sirikasemsuk et al., (2020;2021;2022) investigated the thermal cooling characteristic of the battery module with the thermoelectric cooling module with nanofluid as an in-direct coolant (Hot side flow channel). The present study has been done continuously by using ferrofluid and water as direct coolants flowing into the cylindrical battery pack with different flow directions. The ferrofluid and water have been used as the direct coolant for the battery module (Flow in the cold side flow channel of the thermoelectric cooling module). They are widely used in many applications. Therefore, the sixty 18650 cylindrical Li-ion cells are tested with charge and discharge processes which are directly chilled by ferrofluid flowing through a newly designed cooling system with the different flow directions of coolants.

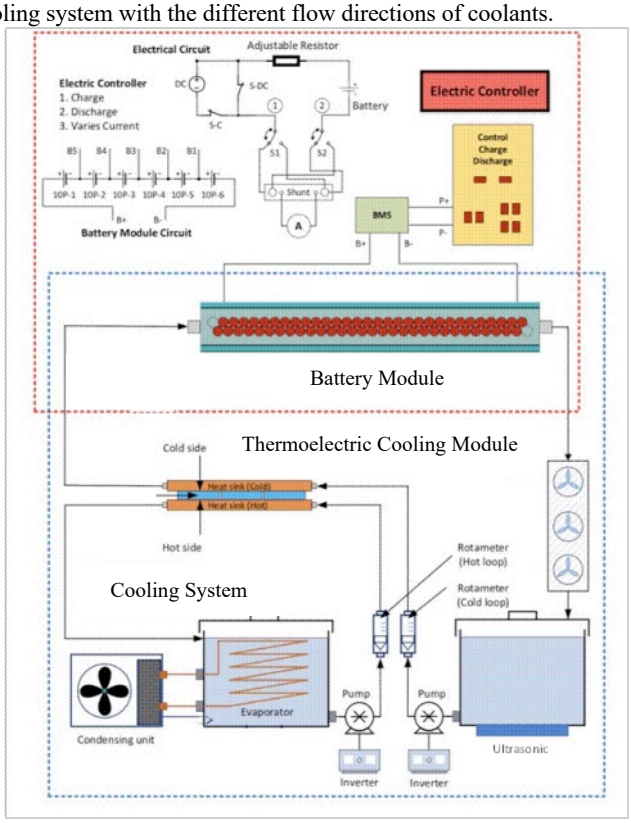

Fig. 1 Schematic diagram of the experimental apparatus

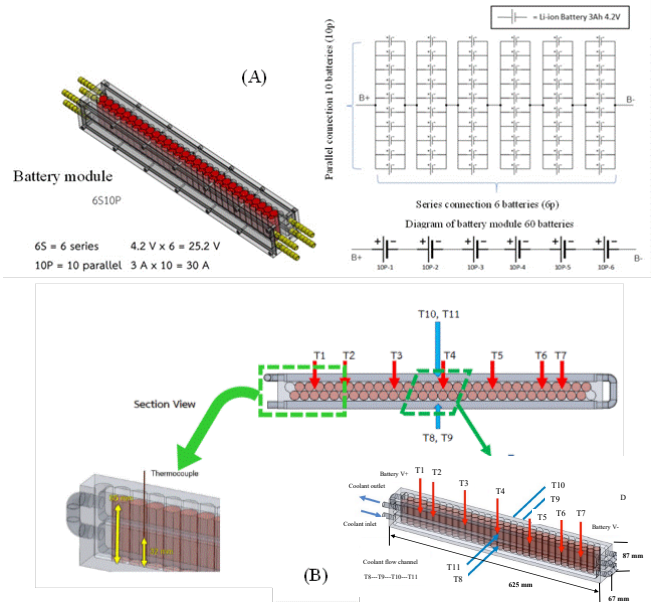

Fig. 2 Details of (A) the battery connection and (B) temperature measurement positions

Global Digital Central
ISSN: 2151-8629

Table 1. Uncertainty and accuracy of the instruments.

Instruments	Accuracy	Uncertainty
Voltage supplied by power source, voltage	0.20%	±0.50
Current supplied by power source, ampere	0.20%	±0.50
Digital weight scale, gram	0.01%	±0.01
Thermocouple type T, Data logger, ºC	0.10%	±0.10

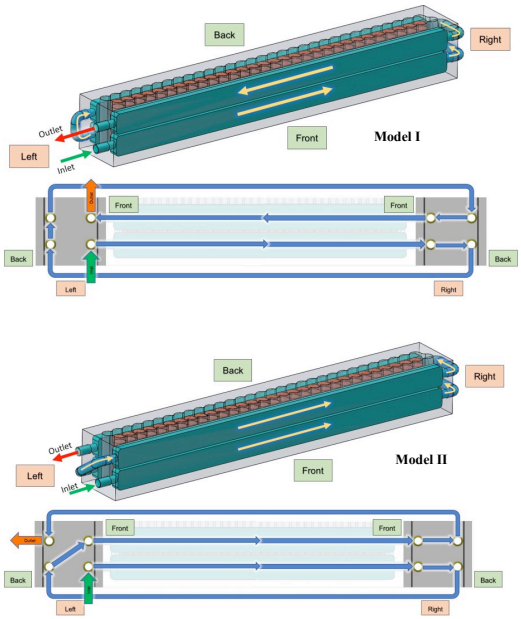

Fig. 3 Details of the coolant flow direction for different battery cooling modules

2. TEST APPARATUS AND PROCEDURE

2.1. Test apparatus

The test systems, R134a refrigeration cooling system, cold side coolant system, hot side cooling system, and electrical control system, are demonstrated in Figure 1. The generated heat is chilled by the ferrofluid coolant entering the jacket flow channel of the battery module. It enters the cooling heat exchanger (radiator) to decrease temperature and flows into the cold-side flow channel of the thermoelectric cooling module to keep constant inlet ferrofluid coolant temperature before entering the pack. However, the hot-side flow channel of the thermoelectric cooling module (TCM) is chilled by water, which is chilled by the refrigeration system for the next cooling loop, as shown in Figure 1. The details of the thermoelectric cooling module can be read from Sirikasemsuk et al., (2020;2021;2022). The ferrofluid coolant flow rate monitoring can be adjusted by a floating flowmeter, while the digital weight scale-with-stopwatch method measures an actual mass flow. The flow rate variation is recorded three times to repeat the measured data. In addition, the accuracy and uncertainty of the instruments are listed in Table 1.

2.2. The liquid cooling system of the battery pack

The 18650 types with the cylindrical shape of the pack and with the liquid system are tested. For the cylindrical battery module of the tesla, EV consists of 16 modules, 444 cylindrical battery cells, and eight-row for each module. For this study, only a row of the battery is used in the experiment, which consists of 60 batteries and the liquid cooling package. The cylindrical Li-ion batteries arrangement consists of six rows, and each row consists of ten cells. Ten cells in each row are a series connection, and each battery row is a parallel connection, as shown in Fig. 2(A). The total voltage and ampere of the pack are 25.2V and 30A.

More details of the two-pole connection can be seen in Sirikasemsuk et al., 2020). The digital control circuit controls the supplied voltage and current for the charged and discharged processes, which changes the connection or disconnection time through the LabVIEW. The power supply connected to the electrical battery pack can be controlled through the battery management system (BMS). The relevant instruments for measuring the various parameters are pre-calibrated with the standard calibrator. As shown in Fig. 1, the electrical circuit designed for this experiment can adjust the current as needed within the device operating range. In addition, there is a device in the electric control cabinet to read the battery capacity, battery voltage, and current.

The details of the cooling system are found in Sirikasemsuk et al., (2020). In the present study, two different flow directions are tested, as in Fig. 3. For model I, the working fluid enters the cooling jacket at the front lower flow channel, rear lower flow channel, and front upper flow channel and then into the rear upper flow channel. For model II, the coolant enters the cooling jacket at the front lower flow channel, rear lower flow channel, and back upper flow channel and then into the front upper flow channel.

All thermocouples are connected to the Datataker DT85, which is linked to the personal computer. All type-T thermocouples are pre-calibrated with a dry block type calibrator and are installed for measuring the cell temperature of the pack for the inlet zone (T1-T3), the middle zone (T4-T5), and the outlet zone (T6-T7). The coolant temperatures are measured at the central zone of each flow channel; the front below channel (T8), the back below channel (T9), the front top channel (T10), and the back top channel (T11), as shown in Fig. 2.

2.3. Ferrofluid preparation

Iron-oxide nanoparticles (Fe_3O_4) with properties as shown in Table 2 are applied as the nanoparticles suspending the water (Ferrofluid) with a concentration of 0.015% by volume. The uniform suspending of nanoparticles is performed continuously by an ultrasonic bath (DELTA) until the obtained stable solution. The ultrasonic bath is held on On-mode for 20 minutes each hour to keep the solution stable during the experiment. The %transmittance spectrum for the first and after two days of the ferrofluid is measured using the Spectrophotometer UV-1800 (Shimadzu, Kyoto, Japan). It is found that the %transmittance spectrum at first and the two days are similar and give an error of 0.92%, which means that the ferrofluids still maintain good stability (Sirikasemsuk et al., 2020). The proposed correlations (Pak et al., 1998, Xuan et al., 2000, Drew et al., 1999, Maxwell, 1881) for calculating the ferrofluid properties are as follows.

$$\rho_{nf} = \varphi\rho_P + (1-\varphi)\rho_w \quad (1)$$

$$\mu_{nf} = (1+2.5\varphi)\mu_w \quad (2)$$

$$\left(\rho C_p\right)_{nf} = \phi\left(\rho C_p\right)_p + (1-\phi)\left(\rho C_p\right)_w \quad (3)$$

$$k_{nf} = \left[\frac{k_p+2k_w-2\varphi(k_w-k_p)}{k_p+2k_w+\varphi(k_w-k_p)}\right]k_w \quad (4)$$

Table 2. Thermo-physical properties of Fe_3O_4 (Shan et al., 2013).

Properties	Values at 25±1
Density, (kg/m^3)	5180
Thermal conductivity, (W/m.K)	80.4
Viscosity, (mPa S)	-
Specific heat, (J/kg.K)	670
Purity, %	>99.9
Average diameter, nm	23

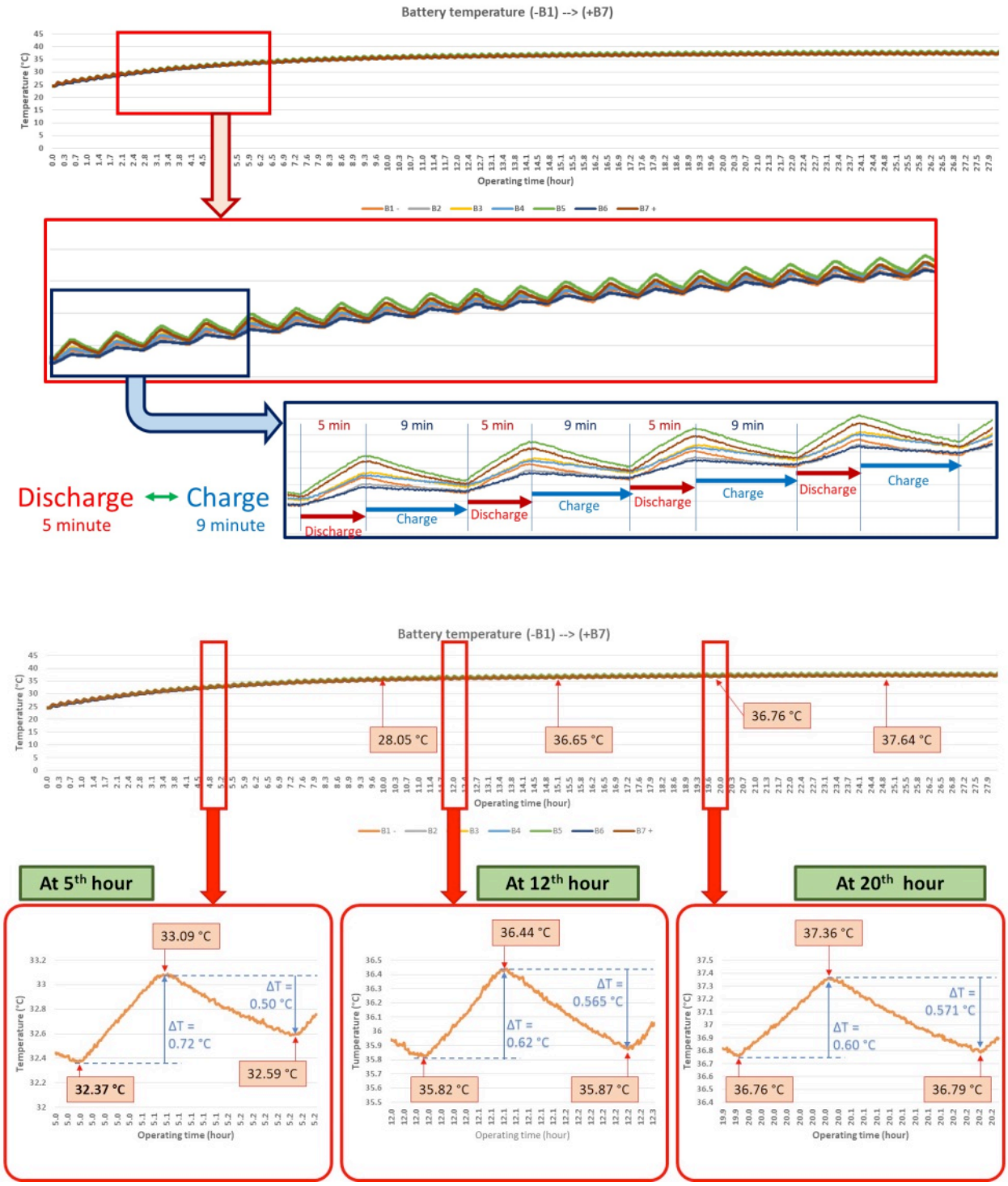

Fig. 4 Variations of battery cells temperature at various positions for charged and discharged processes without cooling

Global Digital Central
ISSN: 2151-8629

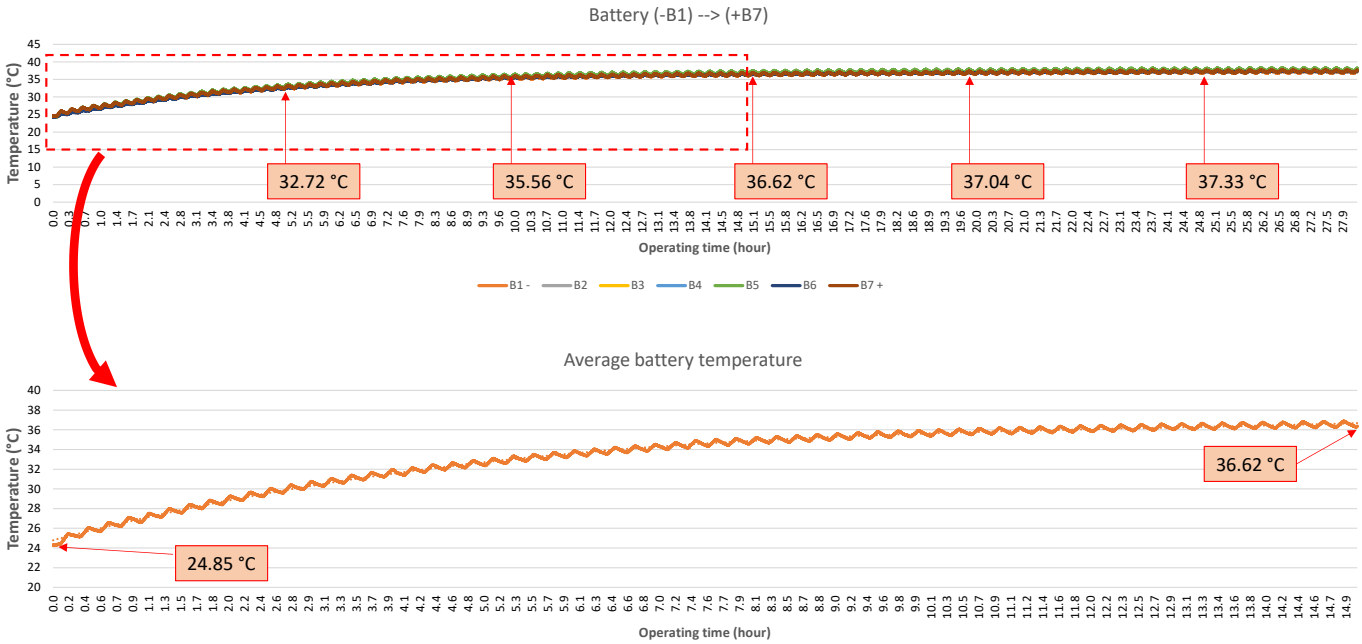

Fig. 5 Variations of average battery temperature

2.4 Experimental test method

First of all, the electrical system and the relevant systems must be safety tested. The surrounding temperature significantly affects the cooling efficiency. Therefore, the whole experiment setup and testing are performed in the air conditioning room (25ºC). For the experimental process, the experimental approaches have been made by operating the battery module without coolant circulation to consider the generated heat of the pack with operating time. The operating conditions are the trickle method (A battery charger that delivers a very low voltage) for the charged process and 4A for the discharged process.

In the experiment, multiply charged, and discharged processes are required to consider the generated heat of the battery module. Therefore, for the stability of the battery cells, controlling the battery module must control the charged and discharged time. The initial current is set to 4A, and the maximum voltage of 100 SOC is 25.2V, while a minimum voltage of 0 SOC is 18V. For a given hot and cold side coolant fluids flow rate and voltage provided into the TCM, the pack has been operated for the multiple charged and discharged processes. The variation of the relevant parameters with the operating time is recorded three times to repeat the measured data.

3. RESULTS AND DISCUSSION

The experiment is performed in the air conditioning room with a constant temperature of 25ºC to decrease the outside air temperature variation effect. For the operating conditions of the battery pack, the charging process has been done under the trickle method (A battery charger that delivers a very low voltage) and the 4A current rate for the discharged process. In real-life conditions, the battery pack must be operating with multiply charged and discharged processes. Due to the internal resistance, the charged process takes longer than the discharged process. The charging time of the battery pack is 9 minutes for 100% battery capacity and 5 minutes for discharging time. The transition between the charged and discharged processes will delay 0.5 seconds, controlled with LabVIEW. Experiments have been performed with two different coolant flow directions, as shown in Fig. 3. First, the pack is controlled with multiple charged and discharged processes without coolant circulation. Without coolant circulation, the generated heat moves from the cells to the cooling battery cooling jacket by conduction mode and accumulates in the jacket. It is found that the cell battery temperature in the middle zone is the highest value and tends to decrease for other positions. In higher operating loops (Charged and discharged processes), the battery pack temperatures at various positions continuously increase with operating time. For the battery pack, the typical reaction between two poles reaction significantly affects the cell reaction during operation. The reaction is endothermic for the charged process and exothermic for the discharged process. Therefore, the temperature tends to decrease for the charged process and increase for the discharged process, as shown in Fig. 4. The total battery cell temperature increases with increasing operating time but is still less than 40ºC. Generally, the pack stability and safety are obtained as the pack is operated at a temperature of less than 40ºC (Heubner et al., 2015). During the operation, the two heat modes are generated (Bernardi et al., 1985). The reaction heat is caused by lithium-ion embedding on/off between two poles. For the charged and discharged processes, the reactions are endothermic reactions and exothermic reactions, respectively. Generally, the generated heat from the battery is divided into two modes: reversible and irreversible. Reversible heat mode is produced from entropy change inside the battery, and overpotential resistance and electrical resistance cause the irreversible mode (Bernardi et al., 1985) as follows;

$$Q = \pm I(U_{ca} - U_{an} - U) - I\left(T\frac{d(U_{ca}-U_{an})}{dT}\right) \quad (5)$$

$I(U_{ca}\text{-}U_{an}\text{-}U)$ is the heat mode due to entropy change, and the second term is the irreversible heat mode due to electrical resistance, and the details can be seen in Heubner et al., (2015), Bernardi et al., (1985), and Nazari et al., (2017). The liquid cooling system is chilled directly using a ferrofluid. Therefore, there are no previously published data to validate the measured data. However, the changing temperature trends during the operation are similar to the previously published results (Pesaran, 2002). The cell temperature significantly increases with operating time. However, as the operating time is > 10 hrs, the battery cell temperature slightly rises. Based on the present results, the relationship between the increasing battery temperature and the operating time, in the operating time of 15 hrs (Fig. 5), is proposed as in the following;

$$T = (2\cdot10^{-12})t^3 - (1\cdot10^{-7})t^2 - 0.0019t + 24.79 \quad (6)$$

The application range is $0 < t < 15$ hr and gives $R^2 = 0.9961$.

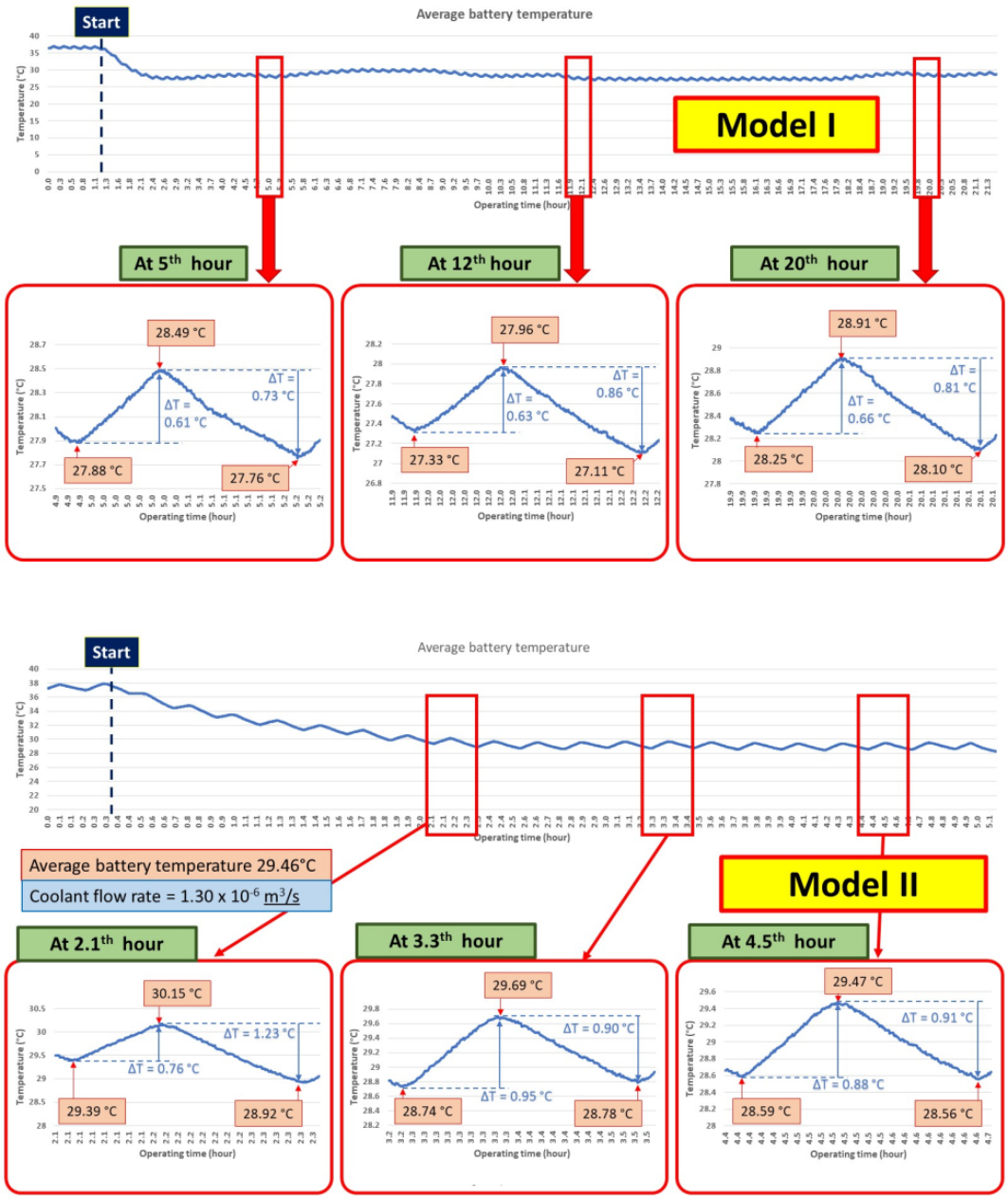

Fig. 6 Variations of average battery temperature for charged and discharged processes with cooling for different battery cooling models

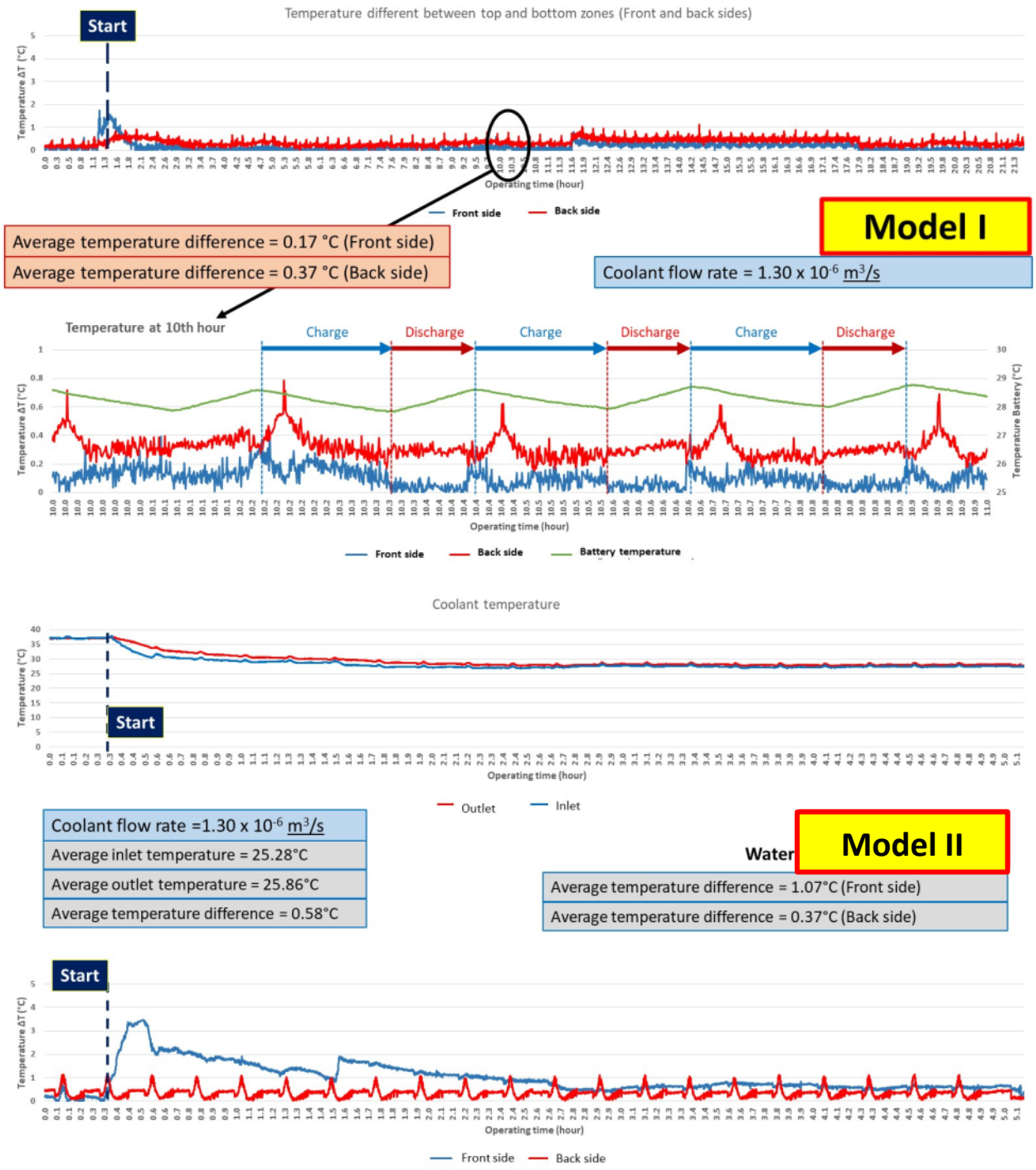

Fig. 7 Variations of the temperature difference between the upper and lower zone of cell battery for different battery cooling models

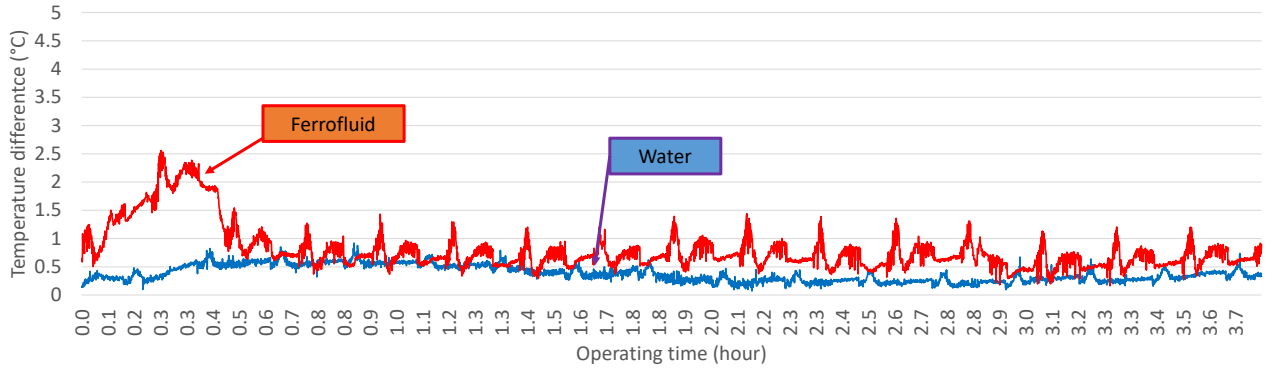

Fig. 8 Variations of the inlet and outlet temperature difference for different coolant types of battery cooling model I

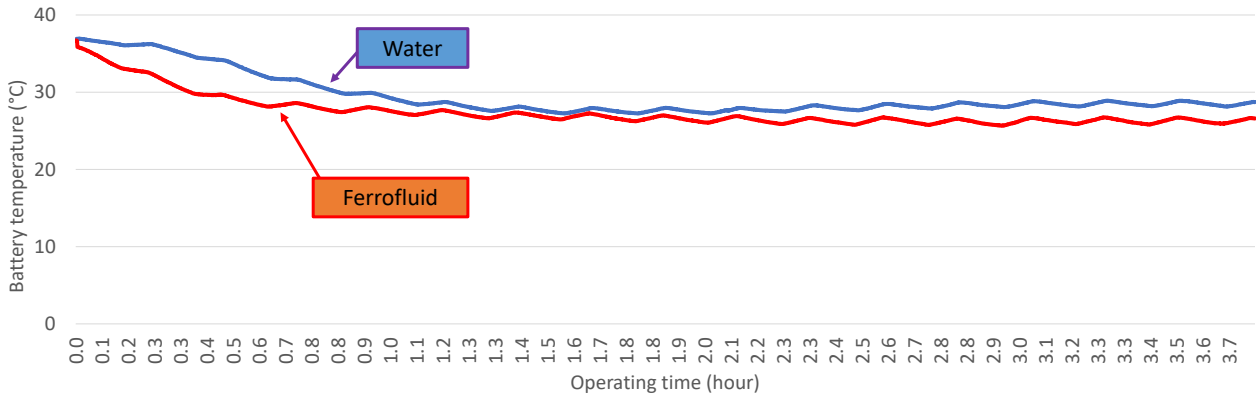

Fig. 9 Variations of average battery temperature for battery cooling model I

Figure 6 shows the average battery temperature with the circulation of the coolant. The Battery pack is operated (multiply charged and discharged processes), and the temperature increases and nearly reaches 38°C, and then the coolant circulation is operated. The liquid circulation significantly affects the heat removal ability, reducing the temperature and giving values less than 30°C. However, although the pack temperature decreases with operating time for the coolant circulation, the changing battery cell temperature during the multiple charged and discharged processes is still similar without coolant circulation. The temperature increase for the discharged process is less than the temperature decrease for the charged process, as shown in Fig. 6. In the cooling system model I and model II, the cell temperatures reduce and decrease to less than 30°C for 2.5 hours after flowing coolant circulation and, after that, nearly constant at about 28.5°C for the model I and 29.46°C for the model II.

In this work, the test procedure has been done with two different flow directions, as shown in Fig. 3. The coolant flow direction significantly affects the cell battery temperature gradient. The temperature gradient across a cell (Both front and back sides) from two cooling models is shown in Fig. 7. At the inlet port zone of the coolant entering the pack (Left-hand side), the minimum temperature is obtained and tends to increase on the other side. This is because of the higher temperature difference for this zone, which results in more cooling capability than different zones. For model I, the maximum temperature gradient across the cell is about 0.17°C for the front side and 0.37°C for the backside, while the model II, the maximum temperature gradient across the cell is about 1.07°C, 0.37°C for the front side and the back side, respectively. This means that the temperature distribution of the cell battery for the cooling model I is better than model II. The decreased temperature gradient across the cell results in a reduced adverse effect. Commercial lithium-ion batteries are subject to temperature fluctuations due to their local environment and operating conditions, and these transient temperatures are well known to impact long-term stability. The adverse effects of temperature shifts show that transitioning from low to higher temperatures can lead to catastrophic failure. In addition, the temperature distribution characteristics for water as coolant are similar to those for ferrofluid as coolant, as shown in Figs. 8, 9. As shown in Fig. 8, the temperature difference between the inlet and outlet for ferrofluid as coolant is higher than those for water as coolant. However, they are less than 1°C. This means that the cooling ability of ferrofluid is higher than water, which results in lower battery pack temperature, as shown in Fig. 9. The suspending nanoparticles promote the Brownian motion, which has a significant effect on the heat transfer enhancement and turbulent intensity. This means that ferrofluids heat removal capability is more effective than their base fluids.

4. CONCLUSION

The battery module must be operated at the designed temperature for higher thermal performance and a longer life cycle. Therefore, the BTMS is significant for chilling. There are many cooling battery direct and indirect methods. In the present study, the battery module with sixty cylindrical cells is chilled using the direct liquid cooling method with two different coolant flow directions. The results showed that the average battery pack temperature increases with increasing operating time without the coolant circulation process. The temperature difference between the upper and lower zones across a cell is 0.27°C, and 0.72°C, for model I and model II, respectively. The decreased temperature gradient across the cell reduces the adverse effect of temperature, which can reduce the failure of the cells. The average battery temperature obtained from model I is 1°C lower than that from model II. This means

Global Digital Central
ISSN: 2151-8629

that cooling model I is better than cooling model II. In addition, the thermal cooling enhancement for ferrofluid as coolant is 4.2% more than for de-ionized water as coolant. However, the optimized condition with the coolant circulation, a larger scale of the battery pack, and different operating conditions have been performed for more extensive thermal performance and a more significant long lifecycle.

NOMENCLATURES

C_p	specific heat capacity, (kJ kg^{-1} ^{o}C)
I	current, [ampere]
k	thermal conductivity, (W m^{-1} ^{o}C^{-1})
T	temperature, (^{o}C)
t	time, (hr)
U	open circuit potential, (voltage)
Greek symbols	
φ	volume fraction, (%)
ρ	density, (kg m^{-3})
μ	viscosity, (Pa s)
Subscripts	
nf	nanofluid
p	particle
w	water
ca	cathode
an	anode
Acronyms	
BMS	battery management system
C-rate	discharge/charge rate relative to maximum capacity
EV	electrical vehicle
PCM	phase change material
SOC	state of charge
TCM	thermoelectric cooling module

ACKNOWLEDGMENTS

This work has been supported by a Srinakharinwirot University (SWU) fund. The authors would like to express their appreciation.

REFERENCES

Abada, S., Marlair, G., Lecocq, A., Petit, M., Moynot, V.S., and Huet, F., 2016, "Safety focused modeling of lithium-ion batteries: A review," *Journal of Power Sources*, **306**, 178-192. https://doi.org/10.1016/j.jpowsour.2015.11.100.

Amietszajew, T., McTurk, E., Fleming, J., and Bhagat, R., 2016, "Understanding the limits of rapid charging using instrumented commercial 18650 high-energy Li-ion cells," *Electrochimica Acta,* **263**, 346-352. https://doi.org/10.1016/j.electacta.2018.01.076.

Bernardi, D., Pawlikowski, E., and Newman, J., 1985, "A general energy balance for battery systems," *J. Electrochemistry Soc*., **132**, 5–12. https://doi.org/10.1149/1.211379.

Bolsinger, C., and Birke, K.P., 2019, "Effect of different cooling configurations on thermal gradients inside cylindrical battery cells," *Journal of Energy Storage*, **21**, 222–230. https://doi.org/10.1016/j.est.2018.11.030.

Budiman, A.C., Hasheminejad, S.M., Sudirja, A., Mitayani, A., and Winoto, S.H., 2022, "Visualization of induced counter-rotating vortic for electric vehicles battery module thermal management," *Frontiers in Heat and Mass Transfer*, **19**. https://doi: 10.5098/hmt.19.9

Chen, A., and Sen, P., 2016, "Advancement in battery technology: A State-of-the-Art Review," *IEEE 2016-ESC-0713*, 1-10. https://doi: 10.1109/IAS.2016.7731812

Chen, D., Jiang, J., Kim, G.H., Yang, C., and Pesaran, A., 2016, "Comparison of different cooling methods for lithium ion battery cells," *Applied Thermal Engineering*, **94**, 846–854. https://doi.org/10.1016/j.applthermaleng.2015.10.015.

Chen, J.L., Li, X.H., Wang, Z.X., and Guo, H.J., 2017, "Mechanism for capacity fading of 18650 cylindrical lithium ion batteries," *Trans. Nonferrous Met. Soc. China*, **27**, 1602−1607. https://doi.org/10.1016/S1003-6326(17)60182-1.

Chen, K., Chen, Y., Li, Z., Yuan, F., and Wang, S., **2018**, "Design of the cell spacings of battery pack in parallel air-cooled battery thermal management system," *International Journal of Heat and Mass Transfer,* 127, 393–401. https://doi.org/10.1016/j.ijheatmasstransfer.2018.06.131.

Chen, K., Song, M., Wei, W., and Wang, S., 2018, "Structure optimization of parallel air-cooled battery thermal management system with U-type flow for cooling efficiency improvement," *Energy*, **145**, 603-613. https://doi.org/10.1016/j.energy.2017.12.110.

Chen, K., Wang, S., Song, M., and Chen, L., 2017, "Configuration optimization of battery pack in parallel air-cooled battery thermal management system using an optimization strategy," *Applied Thermal Engineering*, **123**, 177–186. https://doi.org/10.1016/j.applthermaleng.2017.05.060.

Chen, K., Wang, S., Song, M., and Chen, L., 2017, "Structure optimization of parallel air-cooled battery thermal management system," *International Journal of Heat and Mass Transfer*, **111**, 943–952. https://doi.org/10.1016/j.ijheatmasstransfer.2017.04.026.

Chen, Z., Sun, H., Dong, G., Wei, J., and Wu, J., 2019, "Particle filter-based state-of-charge estimation and remaining-dischargeable-time prediction method for lithium-ion batteries," *Journal of Power Sources*, **414**, 158–166. https://doi.org/10.1016/j.jpowsour.2019.01.012.

Deng, Y., Feng, C., Jiaqiang, E., Zhu, H., Chen, J., Wen, M., and Yin, H., 2018, "Effects of different coolants and cooling strategies on the cooling performance of the power lithium ion battery system: A review," *Applied Thermal Engineering*, **142**, 10–29. https://doi.org/10.1016/j.applthermaleng.2018.06.043.

Drake, S.J., Wetz, D.A., Ostanek, J.K., Miller, S.P., Heinzel, J.M., and Jain, A., 2014, "Measurement of anisotropic thermophysical properties of cylindrical Li-ion cells," Journal of Power Sources, **252**, 298-304. https://doi.org/10.1016/j.jpowsour.2013.11.107.

Drew D.A., and Passman, S.L., 1999, "Theory of multicomponent fluids," *Springer*, Berlin.

Erb, D.C., Kumar, S., Carlson, E., Ehrenberg, I.M., and Sarma, S.E., 2017, "Analytical methods for determining the effects of lithium-ion cell size in aligned air-cooled battery packs," *Journal of Energy Storage*, **10**, 39–47. https://doi.org/10.1016/j.est.2016.12.003.

Feng, X., He, X., Ouyang, M., Lu, L., Wu, P., Kulp, C., and Prasser, S., 2015, "Thermal runaway propagation model for designing a safer battery pack with 25 Ah LiNixCoyMnzO2 large format lithium ion battery,"

Global Digital Central
ISSN: 2151-8629

Applied Energy, **154**, 74–91. https://doi.org/10.1016/j.apenergy.2015.04.118.

Feng, X., Ouyang, M., Liu, X., Lu, L., Xia, Y., and He, X., 2018, "Thermal runaway mechanism of lithium ion battery for electric vehicles: A review," Energy Storage Materials, **10**, 246–267. https://doi.org/10.1016/j.ensm.2017.05.013.

Galatro, D., Al-Zareer, M., Da Silva, C., Romero, D.A., and Amon, C.H., 2020, "Thermal behavior of lithium-ion batteries; aging, heat generation, thermal management and failure," *Frontiers in Heat and Mass Transfer*, **14**. https://doi: 10.5098/hmt.14.17

Ghiji, M., Burch, I., Suendermann, B., Gamble, G., Novozhilov, V., Joseph, P., and Moinuddin, K., 2021, "Lithium-ion fire suppression using water mist systems," *Frontiers in Heat and Mass Transfer*, **17**. https://doi: 10.5098/hmt.17.13

Heubner, C., Schneider, M., Lämmel, C., and Michaelis, A., 2015, "Local heat generation in a single stack lithium ion battery cell," *Electrochimistry Acta*, **186**, 404–412. https://doi.org/10.1016/j.electacta.2015.10.182.

Hong, S., Zhang, X., Chen, K., and Wang, S., 2018, "Design of flow configuration for parallel air-cooled battery thermal management system with secondary vent," *International Journal of Heat and Mass Transfer*, **116**, 1204–1212. https://doi.org/10.1016/j.ijheatmasstransfer.2017.09.092.

Jaguemont, J., Omar, N., Monem, M.A., Bossche, P.V., and Mierlo, J.V., 2018, "Fast-charging investigation on high-power and high-energy density pouch cells with 3D-thermal model development," *Applied Thermal Engineering*, **128**, 1282–1296. https://doi.org/10.1016/j.applthermaleng.2017.09.068.

Jarrett, A., and Kim, Y., 2014, "Influence of operating conditions on the optimum design of electric vehicle battery cooling plates," *Journal of Power Sources*, **245**, 644-655. https://doi.org/10.1016/j.jpowsour.2013.06.114.

Jiaqiang, E., Han, D., Qiu, A., Zhu, H., Deng, Y., Chen, J., Zhao, X., Zuo, W., Wang, H., Chen, J., and Peng, Q., 2018, "Orthogonal experimental design of liquid-cooling structure on the cooling effect of a liquid-cooled battery thermal management system," *Applied Thermal Engineering*, **132**, 508–520. https://doi.org/10.1016/j.applthermaleng.2017.12.115.

Kitagawa, Y., Kato, K., and Fukui, M., 2014, "Analysis and experimentation for effective cooling of Li-ion batteries," *Procedia Technology*, **18**, 63–67. https://doi.org/10.1016/j.protcy.2014.11.014.

Larsson, F., Bertilsson, S., Furlani, M., Albinsson, I., and Mellander, B.E., 2018, "Gas explosions and thermal runaways during external heating abuse of commercial lithium-ion graphite-LiCoO2 cells at different levels of ageing," *Journal of Power Sources,* **373**, 220–231. https://doi.org/10.1016/j.jpowsour.2017.10.085.

Li, K., Yan, J., Chen, H., and Wang, Q., 2018, "Water cooling based strategy for lithium ion battery pack dynamic cycling for thermal management system," *Applied Thermal Engineering*, **132**, 575–585. https://doi.org/10.1016/j.applthermaleng.2017.12.131.

Liu, H., Wei, Z., He, W., and Zhao, J., 2017, "Thermal issues about Li-ion batteries and recent progress in battery thermal management systems: A review," *Energy Conversion and Management,* **150**, 304–330. https://doi.org/10.1016/j.enconman.2017.08.016.

Lu, Z., Meng, X.Z., Wei, L.C., Hu, W.Y., Zhang, L.Y., and Jin, L.W., 2016, "Thermal management of densely-packed EV battery with forced air cooling strategies," *Energy Procedia*, **88**, 682 – 688. https://doi.org/10.1016/j.egypro.2016.06.098.

Lu, Z., Yu, X., Wei, L., Qiu, Y., Zhang, L., Meng, X., and Jin, L., 2018, "Parametric study of forced air cooling strategy for lithium-ion battery pack with staggered arrangement," *Applied Thermal Engineering*, **136**, 28–40. https://doi.org/10.1016/j.applthermaleng.2018.02.080.

Malik, M., Dincer, I., Rosen, M.A., Mathew, M., and Fowler, M., 2018, "Thermal and electrical performance evaluations of series connected Li-ion batteries in a pack with liquid cooling," *Applied Thermal Engineering*, **129**, 472–481. https://doi.org/10.1016/j.applthermaleng.2017.10.029.

Maxwell, J.C., 1881, "A Treatise on electricity and magnetism," *Clarendon Press*, Oxford University, UK.

Mousavi, M., Hoque, S., Rahnamayan, S., Dincer, I., and Naterer, G.F., 2011, "Optimal design of an air-cooling system for a Li-ion battery pack in electric vehicles with a genetic algorithm," *IEEE*, 1848-1855. https://doi: 10.1109/CEC.2011.5949840.

Nazari, A., and Farhad, S., 2017, "Heat generation in lithium-ion batteries with different nominal capacities and chemistries," *Applied Thermal Engineering*, **125**, 1501–1517. https://doi.org/10.1016/j.applthermaleng.2017.07.126.

Pak, B.C., and Cho, Y.I., 1998, "Hydrodynamic and heat transfer study of dispersed fluids with submicron metallic oxide particles," *Experiment Heat Transfer*, **11**, 151-170. https://doi.org/10.1080/08916159808946559.

Parhizi, M., Ahmed, M.B., and Jain, A., 2017, "Determination of the core temperature of a Li-ion cell during Thermal Runaway," *Journal of Power Sources*, **370**, 27-35. https://doi.org/10.1016/j.jpowsour.2017.09.086.

Pesaran, A.A., 2002, "Battery thermal models for hybrid vehicle simulations," *J. Power Sources*, **110**, 377-382. https://doi.org/10.1016/S0378-7753(02)00200-8.

Pety, S.J., Tan, M.H.Y., Najafi, A.R., Barnett, P.R., Geubelle, P.H., and White, S.R., 2017, "Carbon fiber composites with 2D microvascular networks for battery cooling," *International Journal of Heat and Mass Transfer*, **115**, 513–522. https://doi.org/10.1016/j.ijheatmasstransfer.2017.07.047.

Rao, Z., Qian, Z., Kuang, Y., and Li, Y., 2017, "Thermal performance of liquid cooling based thermal management system for cylindrical lithium-ion battery module with variable contact surface," *Applied Thermal Engineering*, **123**, 1514–1522. https://doi.org/10.1016/j.applthermaleng.2017.06.059.

Ren, D., Liu, X., Feng, X., Lu, L., Ouyang, M., Li, J., and He, X., 2018, "Model-based thermal runaway prediction of lithium-ion batteries from kinetics analysis of cell components," Applied Energy, **228**, 633–644. https://doi.org/10.1016/j.apenergy.2018.06.126.

Saw, L.H., King, Y.J., Yew, M.C., Ng, T.C., Chong, W.T., and Pambudi, N.A., 2017, "Feasibility study of mist cooling for lithium-ion battery, *Energy Procedia*, **142**, 2592–2597. https://doi.org/10.1016/j.egypro.2017.12.197.

Saw, L.H., Ye, Y., Yew, M.C., Chong, W.T., Yew, M.K., and Ng, T.C., 2017, "Computational fluid dynamics simulation on open cell aluminium

Global Digital Central
ISSN: 2151-8629

foams for Li-ion battery cooling system," *Applied Energy*, **204**, 1489–1499. https://doi.org/10.1016/j.apenergy.2017.04.022.

Shahid, S., and Chaab, M.A., 2018, "Development and analysis of a technique to improve air-cooling and temperature uniformity in a battery pack for cylindrical batteries," *Thermal Science and Engineering Progress,* **5**, 351–363. https://doi.org/10.1016/j.tsep.2018.01.003.

Shan, C., Guanghui, G., and Fangfang, L., 2013, "Study on the performance of LiMn2O4 using spent Zn–Mn batteries as manganese source," *J. Solid State Electrochemical*, **18**, 1495–1502. https://doi.org/10.1007/s10008-013-2311-0.

Sheikh, M., Elmarakbi, A., and Elkady, M., 2017, "Thermal runaway detection of cylindrical 18650 lithium-ion battery under quasi-static loading conditions," *Journal of Power Sources,* **370**, 61–70. https://doi.org/10.1016/j.jpowsour.2017.10.013.

Singh, R., Lapp, G., Velardo, J., Long, P.T., Mochizuki, M., Akbarzadehd, A., Date, A., Mausolf, K., and Busse, K., 2021, "Battery cooling options in electric vehicles with heat pipes," *Frontiers in Heat and Mass Transfer*, **16**. https://doi: 10.5098/hmt.16.2

Sirikasemsuk, S., Wiriyasart, S., and Naphon, P., 2022, "Experimental investigation of the thermal management system of a battery pack using a thermoelectric air-cooling module," *Heat Transfer*, 1-19. https://doi.org/10.1002/htj.22596

Sirikasemsuk, S., Wiriyasart, S., Naphon, N., and Naphon, P., 2021, "Water/Nanofluids Pulsating Flow in Thermoelectric Module for Cooling Electric Vehicle Battery System," *International Journal of Heat and Technology*, **39**, 1618-1626. https://doi.org/10.18280/ijht.390525.

Sirikasemsuk, S., Wiriyasart, S., Naphon, P., and Naphon, N., 2020, "Thermal cooling characteristics of Li-ion battery pack with thermoelectric ferrofluid cooling module," *International Journal of Energy Research*, **45**, 8824–8836. https://doi.org/10.1002/er.6417.

Spinner, N.S., Hinnant, K.M., Mazurick, R., Brandon, A., Rose-Pehrsson, S.L., and Tuttle, S.G., 2016, "Novel 18650 lithium-ion battery surrogate cell design with anisotropic thermophysical properties for studying failure events," *Journal of Power Sources*, **312**, 1-11. https://doi.org/10.1016/j.jpowsour.2016.01.107

Sun H., and Dixon, R., 2014, "Development of cooling strategy for an air cooled lithium-ion battery pack," *Journal of Power Sources*, **272**, 404-414. https://doi.org/10.1016/j.jpowsour.2014.08.107.

Tan, M.H.Y., Najafi, A.R., Pety, S.J., White, S.R., and Geubelle, P.H., 2018, "Multi-objective design of microvascular panels for battery cooling applications," *Applied Thermal Engineering*, **135**, 145–157. https://doi.org/10.1016/j.applthermaleng.2018.02.028.

Taniguchi, S., Shironita, S., Konakawa, S., Samuel, O., Hernandez, M., Sone, Y., and Umeda, M., 2019, "Thermal characteristics of 80 °C storage-degraded 18650-type lithium-ion secondary cells," *Journal of Power Sources*, **416**, 148–154. https://doi.org/10.1016/j.jpowsour.2019.01.087.

Wang, Q., Ping, P., Zhao,X., Chu, G., Sun, J., and Chen, C., 2012, "Review Thermal runaway caused fire and explosion of lithium ion battery," *Journal of Power Sources*, **208**, 210–224. https://doi.org/10.1016/j.jpowsour.2012.02.038.

Wang, S., Li, Y., Li, Y.Z., Mao, Y., Zhang, Y., Guo, W., and Zhong, M., 2017, "A forced gas cooling circle packaging with liquid cooling plate for the thermal management of Li-ion batteries under space environment," *Applied Thermal Engineering*, **123**, 929–93. https://doi.org/10.1016/j.applthermaleng.2017.05.159.

Wilke, S., Schweitzer, B., Khateeb, S., and Hallaj, S., **2017**, "Preventing thermal runaway propagation in lithium ion battery packs using a phase change composite material: An experimental study," *Journal of Power Sources*, 340, 51-59. https://doi.org/10.1016/j.jpowsour.2016.11.018.

Wiriyasart, S., Hommalee, C., Sirikasemsuk, S., Prurapark, R., and Naphon, P., 2020, "Thermal management system with nanofluids for electric vehicle battery cooling modules," *Case Studies in Thermal Engineering*, **18**, 100583. https://doi.org/10.1016/j.csite.2020.100583

Xie, J., Ge, Z., Zang, M., and Wang, S., 2017, "Structural optimization of lithium-ion battery pack with forced air cooling system," *Applied Thermal Engineering*, **126**, 583–593. https://doi.org/10.1016/j.applthermaleng.2017.07.143.

Xu, M., Wang, R., Reichman, B., and Wang X., 2018, "Modeling the effect of two-stage fast charging protocol on thermal behavior and charging energy efficiency of lithium-ion batteries," *Journal of Energy Storage*, **20**, 298–309. https://doi.org/10.1016/j.est.2018.09.004.

Xuan, Y., and Roetzel, S., 2000, "Conceptions of heat transfer correlation of nanofluids," *Int. J. Heat and Mass Transfer*, **43**, 701-3707. https://doi.org/10.1016/S0017-9310(99)00369-5.

Yuan, C., Wang, Q., Wang, Y., and Zhao, Y., 2019, "Inhibition effect of different interstitial materials on thermal runaway propagation in the cylindrical lithium-ion battery module," *Applied Thermal Engineering*, **153**, 39–50. https://doi.org/10.1016/j.applthermaleng.2019.02.127.

Zhang, M., Yang, K., Qin, L., Yao, X., Liu, Q., and Ju, X., 2022, "Research on a novel concept of self-forming air-cooling battery rack," *Frontiers in Heat and Mass Transfer*, **19**. https://doi: 10.5098/hmt.19.13

Zhang, T., Gao, Q., Wang, G., Gu, Y., Wang, Y., Bao, W., and Zhang, D., 2017, "Investigation on the promotion of temperature uniformity for the designed battery pack with liquid flow in cooling process," *Applied Thermal Engineering*, **116**, 655–662. https://doi.org/10.1016/j.applthermaleng.2017.01.069.

Zhao, C., Cao, W., Dong, T., and Jiang, F., 2018, "Thermal behavior study of discharging/charging cylindrical lithium-ion battery module cooled by channeled liquid flow," *International Journal of Heat and Mass Transfer*, **120**, 751–762. https://doi.org/10.1016/j.ijheatmasstransfer.2017.12.083.

Zhao, J., Rao, Z., and Li, Y., 2015, "Thermal performance of mini-channel liquid cooled cylinder based battery thermal management for cylindrical lithium-ion power battery," *Energy Conversion and Management*, **103**, 157–165. https://doi.org/10.1016/j.enconman.2015.06.056.